



## Anodizing Steel in KOH and NaOH Solutions

T. D. Burleigh,<sup>\*z</sup> T. C. Dotson, K. T. Dotson, S. J. Gabay,  
T. B. Sloan, and S. G. Ferrell

Department of Materials and Metallurgical Engineering, New Mexico Tech, Socorro, New Mexico 87801,  
USA

The authors demonstrate that it is possible to anodize steel in either KOH or NaOH solutions and grow an adherent oxide on the steel surface. By varying the temperature, voltage, and electrolyte composition, one may electrochemically grow either an adherent blue-black magnetite layer, a light brown oxide, or a semiadherent dichroic magnetite layer on many different types of steel. The dichroic oxide layers exhibit the different colors of the rainbow depending on the thickness of the layer and the viewing angle. The color is a function of the optical interference for the thin coatings. By selecting a narrow range of temperature, voltage, and electrode spacing, the adherent, blue-black magnetite layer can be grown several microns thick on some carbon steels. These anodized oxides provide corrosion protection and they are also a suitable substrate for bonding organic coatings.  
© 2007 The Electrochemical Society. [DOI: 10.1149/1.2767417] All rights reserved.

Manuscript submitted January 19, 2007; revised manuscript received June 7, 2007. Available electronically August 16, 2007.

Bare steels rust when exposed to neutral pH water, saltwater, or high humidity air. The corrosion products on low carbon steel after atmospheric exposure are flaky and nonadherent rusts that consist of lepidocrocite ( $\gamma\text{-FeOOH}$ ) and goethite ( $\alpha\text{-FeOOH}$ ).<sup>1</sup> There are numerous methods to prevent steel from rusting, and many of them involve a barrier layer between the steel and the environment. This barrier layer can be a sacrificial coating, such as zinc or aluminum, or an organic coating, such as paints, waxes or oils, or a barrier oxide.

Steel can grow a passive oxide film in caustic solutions and in concentrated nitric acid, but not in neutral water, as do aluminum, chromium, and titanium. The high temperature oxide on steel is generally a loose, dendritic growth that tends to spall and is not a protective barrier. However, there are many bluing and blackening processes that have been developed to form thick, protective oxides on steel. The bluing and blackening processes for steel require elevated temperatures and include such processes as the Niter, Carbonia, Oil Blackening, Barffing, Bower-barffing,<sup>2,3</sup> and many other proprietary commercial processes. The common factor in all of these processes is the requirement for high temperatures, 200–500°C. Although magnetite ( $\text{Fe}_3\text{O}_4$ ) is thermodynamically stable at room temperature,<sup>4</sup> the slow kinetics of the Schikorr reaction restrict the formation of magnetite at temperatures below 100°C.<sup>5</sup> A protective film of magnetite<sup>6</sup> can be formed in a boiler for steam generation that operates above 100°C. The weathering steels can also grow a protective oxide during atmospheric exposure. The weathering steels, ASTM A242 (steel with high Cu and P) and ASTM A588 (steel with high Cu, Cr, and Ni), rust during atmospheric exposure, but after several years they form an outer red rust layer, and an inner black protective layer. The inner black layer has been identified by Raman spectroscopy as magnetite ( $\text{Fe}_3\text{O}_4$ ) and hematite ( $\text{Fe}_2\text{O}_3$ ).<sup>1</sup> Once this inner layer forms, further weight loss by the steel is greatly reduced.

There have been many attempts to electrochemically form a protective oxide on steel using an electric current and an electrolyte. Hollis<sup>7</sup> described a process using batteries to drive an electrical current between two steel pieces immersed in hot caustic soda (NaOH) in his 1899 patent. A preservative coating is formed on the steel attached to the positive terminal. Hollis recommended heat treating this coating between 800 and 1400°F (425–760°C) to convert it to a “magnetic oxid” and increase its preservative nature. In 1900, Hollis patented an addition to his process with a cathodic cleaning step prior to the growth of the oxide.<sup>8</sup> In 1906, Hollis patented another addition to his process with a final step of immersing the coated steel in hot oil.<sup>9</sup> Unfortunately, Hollis’s patents were

very vague and broad and did not enable the reader to form high quality oxide films. A 1966 patent by McCarthy was similar to Hollis’s except that McCarthy added organic acids to the caustic solution, and used hotter solutions (115–145°C) and all of his coatings were a loose, brown oxide that could be wiped off to reveal an adherent, brown oxide.<sup>10</sup> McCarthy’s patent did not mention any oxide color besides brown.

Bongartz<sup>11</sup> described a method for coloring stainless steel in KOH solution, but he stated that his method was not applicable to nonstainless grades of steel because on these steels his method provided a “steely gray, porous, unattractive, loosely adhering oxide film.” Recently Fujimoto<sup>12,13</sup> developed processes to color stainless steel with cyclic polarization in sulfuric acid. Fujimoto’s process consisted of anodically dissolving the stainless steel at one potential, then depositing a chromium hydroxide film back onto the surface at a different potential. Coloring stainless steel with a cyclic polarization in sulfuric acid is a completely different process from anodizing carbon steel in a caustic solution at a constant potential.

Baxter and Gorkiewicz made a reference to “anodized steel” in 1986, but their anodizing process was in a hot borate solution that could grow an oxide only 10 nm thick.<sup>14</sup> The purpose of their treatment was to passivate the steel surface so they could then image any fatigue cracks by using a potassium iodide gel.

There have been many reports on the electrochemistry of iron in caustic solutions. Joriet et al. described the oxides formed on iron in 1 M NaOH, but their work dealt with the passive region.<sup>15</sup> The iron-nickel alkaline rechargeable battery relies upon the Fe to  $\text{Fe}_3\text{O}_4$  reaction for the battery’s negative electrode.<sup>16</sup> The battery electrolyte is typically 25–30% KOH with 15 g/L LiOH. There are many similarities between the electrochemistry of the iron–nickel battery and the anodizing process described herein, but for the battery, the initial  $\text{Fe}_3\text{O}_4$  is produced by a high temperature process. The Pourbaix diagrams illustrate that iron oxides and/or hydroxides ( $\text{Fe}_2\text{O}_3$ ,  $\text{Fe}_3\text{O}_4$ ,  $\text{Fe}(\text{OH})_2$ ,  $\text{Fe}(\text{OH})_3$ ) can be in electrochemical equilibrium with water at high potentials and in neutral to basic solutions.<sup>4</sup> The regions of passivity correspond roughly to the regions where  $\text{Fe}_2\text{O}_3$  and  $\text{Fe}(\text{OH})_3$  are thermodynamically stable. However, one cannot predict the thicknesses of the oxides from thermodynamics alone.

The above literature review briefly describes the current knowledge for anodizing steel and the electrochemistry of iron in caustic solutions. The patents by Hollis<sup>7–9</sup> and McCarthy<sup>10</sup> describe the general concepts, they did not enable the reader to grow either the dichroic multicolored films, nor the thick adherent blue-black oxides on steel, which are described in this current paper.

### Experimental

During the course of these experiments, many different steels were anodized in many different solutions. The optimum anodization setup is shown in Fig. 1. The steel to be anodized was con-

\* Electrochemical Society Active Member.

<sup>z</sup> E-mail: burleigh@nmt.edu

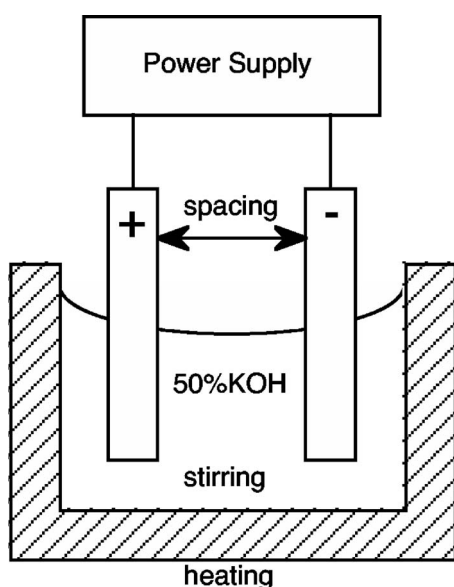


**Figure 1.** To anodize the steel, the steel is polarized positive while immersed in a heated and stirred solution of either KOH or NaOH.

nected to the positive terminal (the anode) of the power supply and a steel counter electrode was connected to the negative terminal (the cathode). For large amperages, a TecNu DCa 25/12-1Z power supply was used which had a maximum capacity of 25 A and 12 V. The TecNu is a two-electrode system, so the voltages are reported for two steel electrodes spaced at either 5, 7, or 9 cm apart. Changing the electrode spacing changed the voltage drop across the solution and the voltage drop across the steel interface. The saturated calomel electrode (SCE) was used sparingly due to concern with contaminating the electrolyte with KCl.

Most of the experimental work reported is on 1010 steel panels (type S-46 Q-Panel). These 1010 steel samples were 15 cm long, 5 cm wide, and 0.8 mm thick. Tests were also conducted on several different steels, including interstitial free steel, weathering steels, and stainless steel. The different types of steel tested and their compositions are given in Table I. The weathering steels, COR-TEN A and B, were 7.6 cm long, 1.3 cm wide, and 1.5 mm thick. The sheet steel samples were tested in the as-received, cold-rolled, surface

condition, while the COR-TEN samples were wet polished to 5 or 1  $\mu\text{m}$  alumina. Before placing the sample in the caustic solution, they were rinsed with deionized water, next rinsed with methanol, and then air dried using compressed air. It was found possible to anodize the steel in KOH or NaOH solutions with concentrations anywhere from 10% to saturated. Most of the tests reported herein were conducted in either 50% KOH or 25% NaOH. The 50% KOH solution was either purchased or prepared by adding deionized water to 500 g of KOH to make 1 L of solution. This concentration is also known as 50% W/V. The 25% NaOH solution was either purchased or prepared by adding deionized water to 250 g of NaOH to make 1 L of solution. After anodization, the sample was removed from the solution, rinsed with deionized water, air dried with compressed air, and then tested. A few samples also had a thermal heat treatment. For the thermal treatment, the anodized sample was placed on the Corning hot plate surface at approximately 450°C until a color change was observed, approximately 15 min.

The electrochemical tests were conducted using a Parstat 2263 potentiostat running PowerSuite software for electrochemical impedance spectroscopy (EIS) or potentiodynamic polarization (PDP). For the PDP test in 50% KOH, a narrow steel sheet was imbedded in epoxy, and polished to 5  $\mu\text{m}$  alumina, to reveal a 2  $\text{mm}^2$  surface area, and was tested in 75 mL of solution. For EIS and PDP in 3.5% NaCl, the corrosion cell was a glass cylinder with an O-ring on the end that was clamped to the anodized steel to form a watertight seal. Approximately 50 mL of saltwater solution were used in these tests. The O-ring had an inside diameter of 2.5 cm, and therefore a testing surface area of approximately 4.9  $\text{cm}^2$ . The reference electrode for these tests was a saturated calomel electrode (SCE).

For salt spray corrosion tests, a thin film of 3.5% NaCl aqueous solution was sprayed onto the samples. The samples were then positioned at a 45° angle in a sealed plastic container. At regular intervals, the samples were observed and a qualitative comparison of the corrosion resistance of the samples was made.

Thin film X-ray diffraction spectra were obtained using the Siemens D500 X-ray diffractometer with a thin film attachment and a Cu K $\alpha$  target. The incident X-ray beam was held at an angle of either 0.5 or 2.0° while the 2-theta diffraction angle was scanned. The 2.0° angle gave a larger signal, but also penetrated much deeper and was not suitable for the very thin anodized films. Both Auger and secondary ion mass spectroscopy (SIMS) were performed using a Perkin-Elmer 4300 Auger Microscope. Scanning electron micrographs were obtained using the Hitachi S-800 field-emission scan-

**Table I.** The compositions of the different steels tested.

Common name	UNS no.	Composition (wt %)								
		Fe	C	Mn	Cu	Ni	Si	Cr	Nb	Other
1010	G10100	Bal	0.09	0.33	0.01	0.01		0.02		0.05 Al
1018	G10180	Bal	0.19	0.67	0.08	0.04	0.02	0.03	0.004	
1215	G12150	Bal	0.07	0.99	0.14	0.04	0.01	0.05	0.001	0.30 S, 0.08 P
4340	G43400	Bal	0.43	0.72	0.15	1.72	0.24	0.82	0.007	0.25 Mo
A572	K02303	Bal	0.07	0.58	0.04	0.01	0.08		0.029	
A36	K02600	Bal	0.15	0.79	0.33	0.15	0.26	0.16	0.004	0.04 Mo
A588	K11430	Bal	0.06	0.91	0.30	0.15	0.40	0.52	0.004	
(COR-TEN B)										
A242	K11510	Bal	0.09	0.36	0.27	0.12	0.39	0.87		0.09 P
(COR-TEN A)										
HY80	K31820	Bal	0.17	0.27	0.14	2.25	0.30	1.25		0.24 Mo
HP stainless	N08705	37.75	0.55	1.23		34.75	1.11	24.3		0.20 Mo
IF steel	G10010	Bal	0.01	0.12					0.024	
1010 (type S-46 Q-panel ground)	G10100	Bal	Max 0.13	0.25–0.60						Max 0.40 P
1010 (type D-46 Q-panel smooth)	G10100	Bal	Max 0.13	0.25–0.60						Max 0.40 P

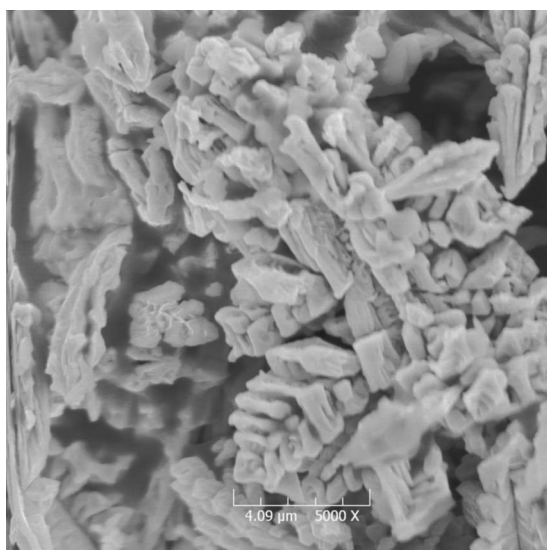


**Figure 2.** The FESEM image shows the dendritic Fe particles which are deposited on the steel counter electrode.

ning electron microscope (FESEM) at New Mexico Tech or the Hitachi S-4800 FESEM at LKO at University Erlangen-Nuremberg in Germany.

### Results and Discussion

Given the proper conditions, the authors found that a thick iron oxide could be grown on the surface of steel by polarizing the steel electrode positive in a hot, stirred, concentrated solution of either KOH or NaOH. By careful control of the temperature and the voltage, one could force a large electric current ( $\sim 30$  to  $\sim 600$  mA/cm<sup>2</sup>) to flow between the positive electrode and the negative electrode, resulting in a thick iron oxide grown on the steel surface. This film which formed on the positive electrode (anode) is referred to as an anodic oxide. As time progressed, the originally clear electrolyte changed to purple and a black deposit formed on the negative electrode (cathode). The next several sections describe these anodizing results in greater detail.

The optimum electrolytes for anodizing were determined to be hot, rapidly stirred solutions of either 50% KOH or 25% NaOH. Solutions of KOH and NaOH, from 10% to saturated, were found suitable to anodize the steel, but different electrolyte compositions also affected the times, temperatures and oxide's properties. (Although steel could be anodized in 5% NaOH, it required  $>2$  A/cm<sup>2</sup> and +12 V.) Besides KOH and NaOH, we did not find any other caustic solutions in which we could anodize the steel. Saturated LiOH solutions would not grow an oxide, even at  $>2$  A/cm<sup>2</sup>, and the steel showed no measurable weight loss. Steel anodized in concentrated NH<sub>4</sub>OH had a negligible current, even at +12 V. Heated solutions of NH<sub>4</sub>OH were not feasible since the NH<sub>4</sub>OH boiled near 40°C. In all other neutral and acid solutions tested, the steel would only dissolve in the transpassive region. For the 50% KOH solution, the anodization was only 1% efficient, that is, only 1% of the current was actually converted into growing the oxide. The remainder of the current evolved hydrogen or oxygen or dissolved Fe and plated it onto the counter electrode as iron dendrites (see Fig. 2). These dendrites were identified as iron by X-ray diffraction, although the iron crystal lattice was slightly expanded possibly due to the substitution of potassium atoms for iron in the lattice. Energy dispersive spectroscopy (EDS) analysis on the FESEM showed the presence of potassium in the iron dendrites. Figure 3 shows the PDP test results for 1010 steel in 50% KOH at room temperature and 70°C, as measured with the PARSTAT 2263. The passive region ( $\sim 0$  V SCE) will only form a 5–10 nm thick film. The anodization process occurs

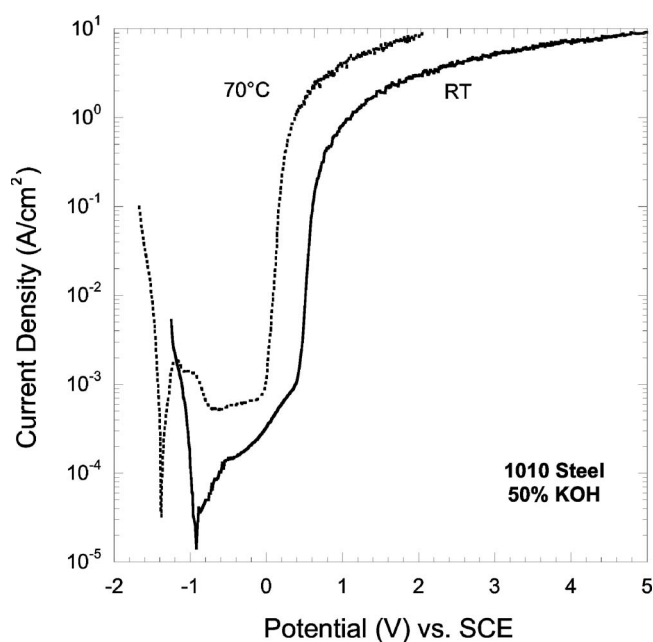


**Figure 3.** PDP tests of 1010 steel in 50% KOH solution indicate a passive region at low potentials, and transpassive region at higher potentials.

on the shoulder of the transpassive region. Changing potentiostats and the experimental setup, however, also changed the current density. The TecNu potentiostat (using 50% KOH at 60°C and 9 cm electrode spacing) with a constant applied +2.0 V vs the steel counter electrode would start at +0.6 V SCE, and decrease to +0.5 V SCE during the first minute, and average 340 mA/cm<sup>2</sup>.

Prior to the anodization, the 50% KOH electrolyte was clear. After several amp minutes, the electrolyte turned violet then dark purple. (This dark purple color was indicative of ferrate ( $\text{FeO}_4^{2-}$ ) or permanganate ( $\text{MnO}_4^-$ ) in the solution.<sup>17</sup> Since the purple color occurred even with 99.9% Fe, it was most likely ferrate.) After the anodization was completed, the solution would return to a light blue ( $\text{HFeO}_2^{-1?}$ ) and then gradually revert back to clear. As the solution was used for longer times, it would remain purple and precipitate red rust ( $\text{Fe}(\text{OH})_3$ ) onto the bottom of the beaker. The used purple solution would grow the anodic oxide faster than a new clear solution. Chemical analysis of the used purple solution showed the presence of 30 ppm Fe still in the solution after several weeks of nonuse. Neutralization of the purple solution with acid would turn the purple solution clear again. If the purple solution was heated above 110°C, it would turn green ( $\text{Fe}^{+3?}$ ), and anodization in the green solution at 120–130°C would grow a gold-brown oxide, similar to that reported by McCarthy.<sup>10</sup> The high temperatures used in McCarthy's patent prevented him from obtaining the dichroic or adherent oxides which are described herein. The organic compounds claimed in McCarthy's patent were found not to be necessary to grow the gold-brown oxides.

Figure 4 shows a sample of 1010 steel anodized in slightly used (light purple) 50% KOH at +2.0 V, 70°C, and raised 1 cm every minute. The brilliant colors of the dichroic oxide are caused by optical interference and are a function of the optical thickness of the film grown on the surface. The refractive index multiplied by the actual thickness of the film gives the optical thickness (Eq. 1).<sup>18</sup> Table II shows how the thickness of the magnetite film grown on the steel was estimated by comparing the color of the magnetite film on steel with the corresponding color of a silica film grown on silicon.<sup>19</sup> The same color on steel and silicon means the same optical thickness of the oxide. (The reasons why this film is believed to be



**Figure 4.** (Color online) The dichroic oxide film as grown on 1010 steel in 1 min increments, in a slightly used (light-medium purple) 50% KOH solution, at 70°C, and +2 V vs the steel counter electrode.

magnetite are given in a later section.) The refractive index of magnetite varies from 2.4 to 2.5 over the visible spectrum,<sup>20</sup> and was approximated to be 2.42<sup>21</sup>

$$n_0 t_0 = n_1 t_1 = \text{optical thickness} \quad [1]$$

Figure 5 shows the growth of the oxide film on 1010 steel in a used (dark purple) 50% KOH at 70°C and +2.0 V. This oxide formation was adherent until about 120 nm, and then it became non-adherent and additional growth could be wiped off with a cotton swab. The thickness (nm) has a cubic relation with time (min), and the empirical fit to the data in Fig. 5 is shown in Eq. 2.

**Table II.** The thickness of the magnetite film grown was estimated from the known relationship between the optical thickness and film thicknesses of silica grown on silicon (see Refs. 18 and 19).

Film thickness (nm)	Color (viewed from directly above)	Film thickness (nm) Anodized steel magnetite, $n = 2.42$
50	Tan	30
70	Brown	40
100	Dark violet to red violet	60
120	Royal blue	70
150	Light blue to metallic blue	90
170	Metallic to very light yellow green	100
200	Light gold or yellow slightly metallic	120
220	Gold with slight yellow-orange	130
250	Orange to melon	150
270	Red-violet	160
300	Blue to violet-blue	180
310	Blue	190
320	Blue to blue-green	195
340	Light green	205
350	Green to yellow-green	210
370	Green-yellow	225
390	Yellow	235
410	Light orange	245
420	Carnation pink	255
440	Violet-red	265
460	Red-violet	280
470	Violet	285
480	Blue-violet	290
490	Blue	295
500	Blue-green	300
520	Green (broad)	315
540	Yellow-green	325
560	Green-yellow	340
570	Yellow to yellowish or creamy gray	345
580	Light orange or yellow to pink	350
600	Carnation pink	360

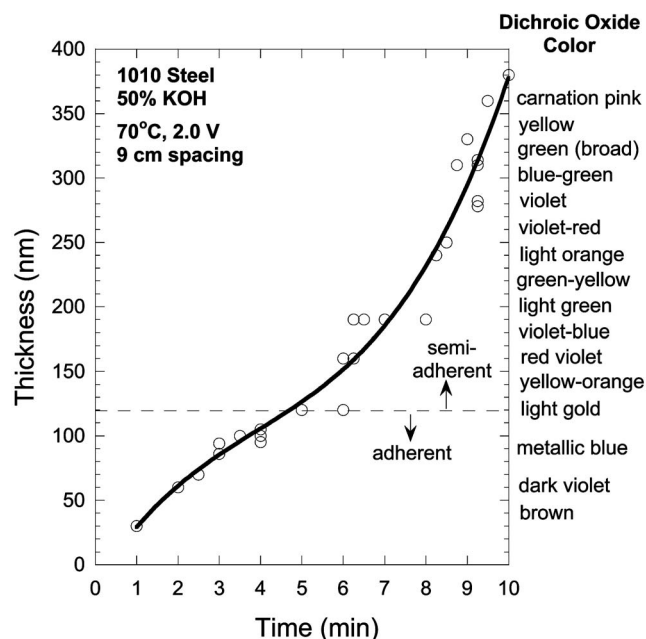


**Figure 5.** The dichroic oxide film grown on 1010 steel in a used (dark purple) 50% KOH solution is adherent up to 120 nm. The color corresponds to the oxide thickness.

$$\text{Thickness} = (-15.3) + (51.5 \times \text{time}) + (-8.04 \times \text{time}^2) + (0.683 \times \text{time}^3) \quad [2]$$

Faster growth rate occurred at higher temperatures, higher voltages, and with greater concentration of impurities in the solution. The used solution would grow an oxide film 50% faster than the new fresh solution, evident in comparing the growth in Fig. 5 vs that in Fig. 4. Very rapid growth also occurred as the temperature was increased. A gold, 120 nm thick, film could be grown in 10 s at 100°C, +4 V and 0.5 A/cm<sup>2</sup>. However, the oxide films were more uniform at 70–90°C temperatures and voltages closer to +2 V. Figure 6 shows that at low voltages (+2.5–2.7 V) in a room temperature solution, the addition of 1–5% NaNO<sub>3</sub> to the 50% KOH also

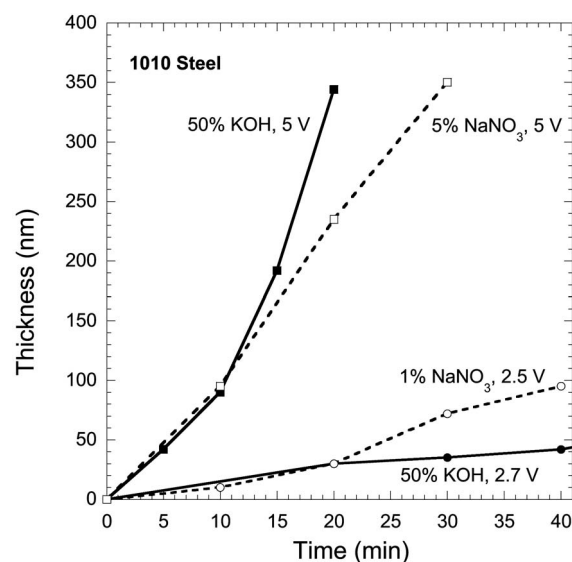


**Figure 6.** Impurities, such as nitrates, have a slight effect on the growth rate of surface oxide on 1010 steel.

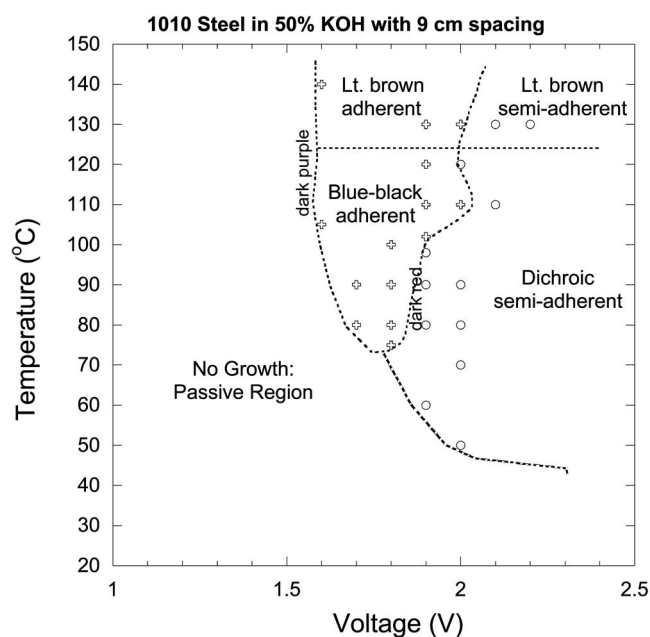


**Figure 7.** The temperature-voltage map for 50% KOH shows the regions for the formation of the different anodic oxide films.

accelerated the growth of the oxide. However, at higher voltages (+5 V), the nitrates apparently retarded the growth of the oxide. Contaminants in the solution do have an effect on the growth rate of the anodic oxides.

Adherent blue-black oxides could be grown several microns thick on the 1010 steel in a narrow region of low voltages and high temperatures in 50% KOH. Figure 7 illustrates that growth at ranges between +1.8 V and 80°C, and +1.6 V and 105°C, could give blue-black oxides several microns thick. (These oxides could *not* be wiped off with a cotton swab.) A similar window for adherent blue-black oxides also existed for 25% NaOH where a thick adherent oxide could be formed at +1.8 V and 80°C, or +2.1 V and 65°C. When the 1010 steel was anodized for 5 min in 25% NaOH with 7 cm spacing, the resulting temperature-voltage map may be seen in Fig. 8. (With increased electrode spacing, the curves would shift to

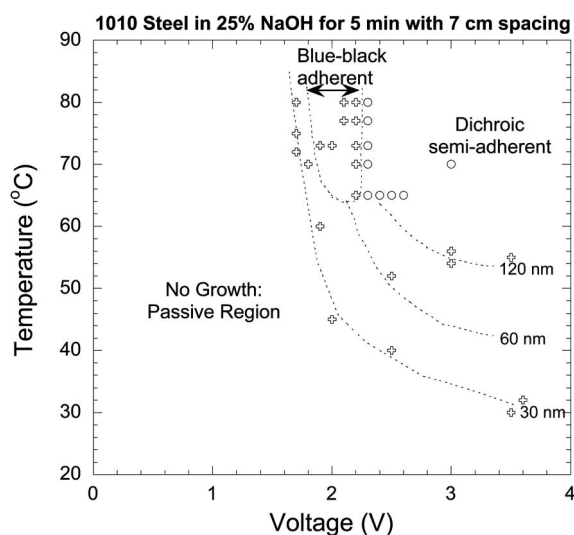


**Figure 8.** The temperature-voltage map for 25% NaOH shows the different anodic oxides formed during 5 min of anodization of the 1010 steel.

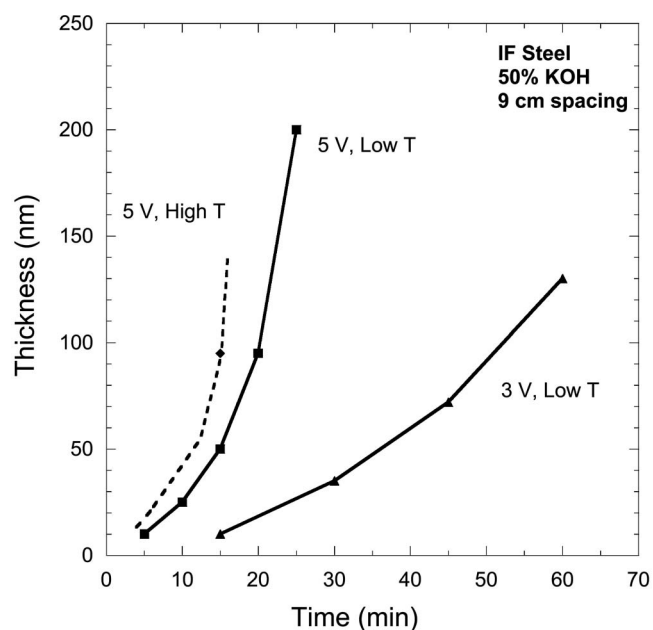


**Figure 9.** Oxide film growth for interstitial free steel anodized in a 50% KOH solution shows faster growth at higher temperatures and/or higher voltages. Although this graph is for interstitial free steel, it is similar for the other carbon steels.

higher voltages.) Anodization in the passive region would result in no growth, while higher voltages would grow a dichroic oxide adherent to only 120 nm. If the electrodes were placed very close (a few centimeters apart), then the nonadherent gold-brown oxide formed on the steel. The anodic oxides grown in the NaOH and KOH solutions were similar, but they formed at different times temperatures and voltages.

All of the steels listed in Table I would anodize at similar rates, with the exception of the stainless steel, HP, which would not anodize, and the COR-TEN steels, which anodized differently as described in a later section. Interstitial free steel (0.01C) was anodized and the results are similar to 1010 steel (0.1C), and are shown in Fig. 9. Figure 9 also illustrates that the faster growth occurred at higher temperatures and voltages. The “low T” referred to tests started at room temperature, and then the solution heated due to joule heating of the solution by the high current density. The “high T” referred to solutions heated to >50°C prior to initiation of the test.

For the weathering steels COR-TEN A (A242) and COR-TEN B (A588) only the dichroic oxide could be grown. We did not find a temperature and voltage range for the blue-black adherent film. Figure 10 shows a broad temperature and voltage range wherein a 200 nm adherent film could be produced on samples of both steels wet polished with 5  $\mu\text{m}$  alumina grit, with the electrodes spaced 5 cm apart. Films thicker than 200 nm were wiped off with a cotton swab. When samples were wet polished with 1  $\mu\text{m}$  alumina, the maximum adherent thickness was reduced to 70 nm, the royal blue color. Thus, the maximum thickness of an adherent oxide grown on these weathering steels appears to be a function of the surface roughness. Although there is a limiting thickness, the anodizing still provides a process to “preweather” these weathering steels in the factory by anodizing them so that they start service with a protective layer and thus not bleed rust for years.

The anodized steel showed improved corrosion resistance over both bare steel and thermally oxidized steel in both salt water spray and in deionized water spray. The anodized plus thermal treated steel showed the greatest corrosion resistance for both the deionized and saltwater spray.

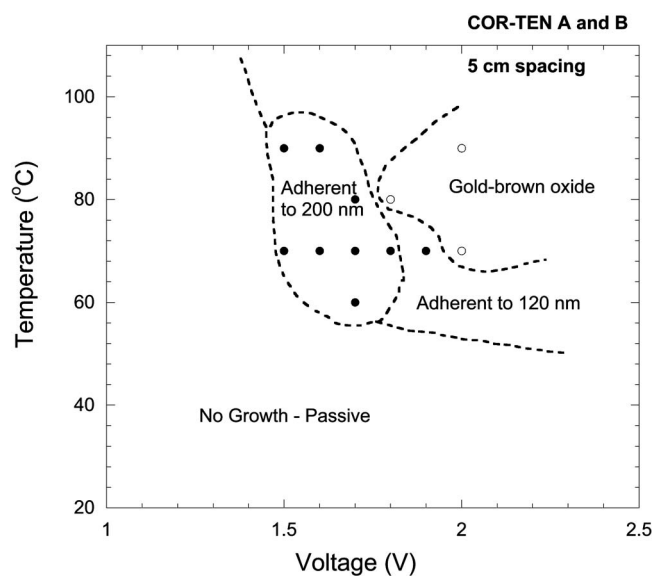


**Figure 10.** The temperature-voltage map of the COR-TEN A and B weathering steels (5  $\mu\text{m}$  polish) anodized in 50% KOH solution.

The Hitachi S-4800 FESEM examination of the top of the blue anodic oxide on 1010 steel revealed the surface to have a fine network of pores with diameters 20–40 nm, as shown in Fig. 11. These pores are ideal for the mechanical bonding of organic coatings, or reservoirs for holding oils, waxes or inhibitors in the surface. Anodized samples that were sprayed with acrylic clear coat and buried in the soil for over a month showed greater corrosion resistance than steel samples that were coated but not anodized, and anodized but not coated.

The Hitachi S-800 FESEM micrograph of the cross section of the blue-green dichroic oxide is shown in Fig. 12. This blue-green oxide is estimated to be 300 nm thick, based on Fig. 5 and Table I. The arrows in Fig. 12 show a 300 nm gap, which agrees very well with the estimated thickness of the oxide. The cross section of the oxide film does not reveal the porosity seen in the top view (Fig. 11) but this could be a function of the sample polishing or differences in the resolution of the two FESEM micrographs. Figure 13 shows the FESEM micrograph of the surface cracking of a thick, dichroic ox-

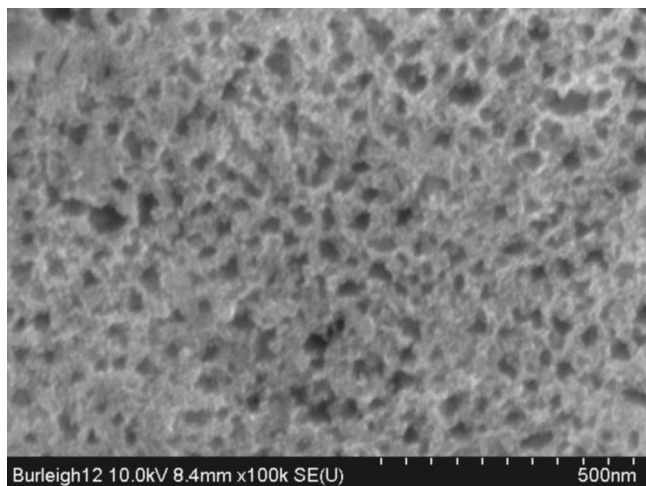


**Figure 11.** FESEM micrograph of blue, 70 nm thick, oxide film formed on 1010 steel in 50% KOH solution shows the oxide surface covered with 20–40 nm sized pores.

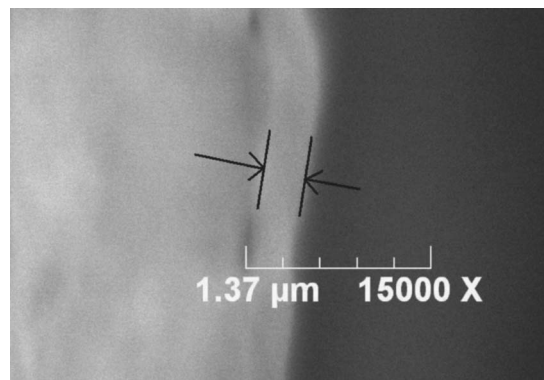
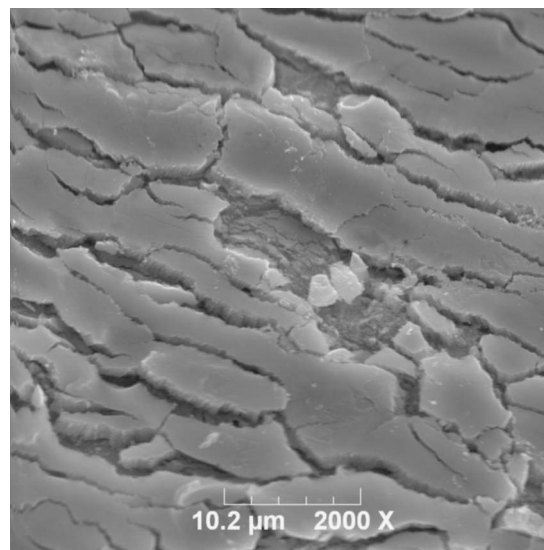


**Figure 12.** The blue-green dichroic oxide is approximately 300 nm thick, which agrees with its optical thickness. (This oxide was grown on 1010 steel in 50% KOH.)

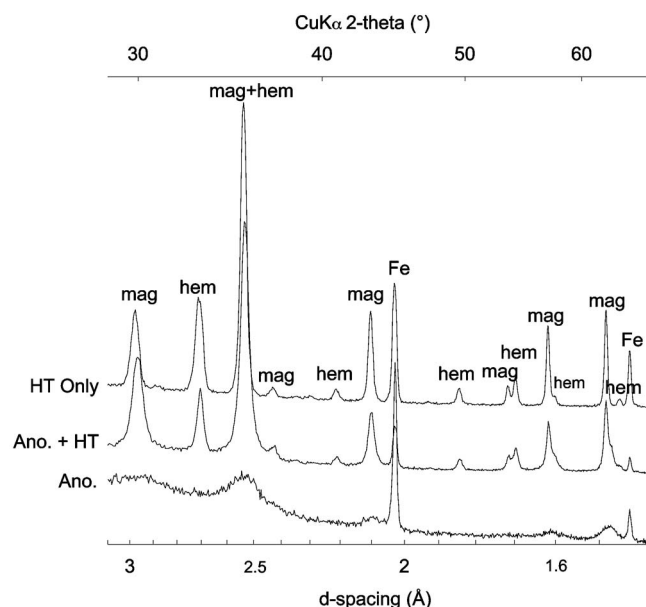
ide on the edge of a steel sheet that was bent 180°. The oxide was very adherent, and showed very little flaking, although it was very brittle.

Figure 14 shows the thin film X-ray diffraction (XRD) scans for the different treatments. Peaks are labeled “mag,” “hem,” or “Fe” corresponding to magnetite, hematite, or iron, respectively. The lowest curve (Ano.) is for the sample that was anodized in 50% NaOH at +1.7 V for 2 h at 50°C, and received no separate heat treatment (HT). This anodized film shows broad “hills” rather than peaks indicating a highly disordered oxide, bordering on amorphous. The sharp Fe peaks are from the substrate. The XRD scans for anodized samples look similar regardless of whether NaOH or KOH solutions were used, or the dichroic or blue-black oxide. The middle curve (Ano. + HT) is for the anodized sample that was heated to about 450°C in air for 10 min. The oxide has formed distinct crystallites as evidenced by the sharp peaks. The top (HT Only) sample was heated to 450°C in air with no prior anodizing treatments. The XRD peaks for the “Ano. + HT” appear similar to the “HT Only” with sharp magnetite and hematite peaks, with relatively more magnetite in the anodized sample.

Determination of whether the oxide grown on the steel was magnetite or maghemite was complicated because the two have nearly



**Figure 13.** The surface oxide is obvious when a 1010 steel sample was crimped in half and the dichroic surface oxide cracked as seen in this FESEM micrograph.



**Figure 14.** XRD spectra for heat treated only (HT only) and anodized and heat treated (Ano. + HT) 1010 steel samples show sharp magnetite (mag) and hematite (hem) peaks in contrast to a sample that was only anodized (Ano.) which has broad magnetite hills.

identical cubic crystal structures, and therefore nearly identical XRD patterns. However, at high diffraction angles ( $86^\circ < 2\theta < 95^\circ$ ), the XRD peaks in the “Ano. + HT” scan corresponded to magnetite ( $\text{Fe}_3\text{O}_4$ ) rather than maghemite ( $\gamma\text{-Fe}_2\text{O}_3$ ). Furthermore, the iron vacancy superlattice peaks, characteristic of maghemite,<sup>22</sup> are noticeably absent. Working backwards, we inferred that the anodic oxides not receiving the heat treatments were also closer to magnetite because a maghemite layer would not convert to magnetite on heating in air.<sup>22</sup> There is also some oxidation of magnetite into hematite ( $\alpha\text{-Fe}_2\text{O}_3$ ), a hexagonal crystal structure, which grows on the outer surface of the magnetite.<sup>23</sup> From Sherrer’s equation the crystallite sizes in the heat treated, anodized films were roughly 30–50 nm based on the XRD peak broadening.<sup>24</sup> The magnetite peak at  $2.10 \text{ \AA}$  ( $43.0^\circ$ ) had a peak broadening that varied from 4 to 6 mrad. The iron peak at  $2.03 \text{ \AA}$  ( $44.6^\circ$ ) was used as a reference. Based on thermodynamic considerations,<sup>25</sup> we inferred that the anodized, unheated oxides are magnetite as well, albeit with a much smaller crystallite size of a few nanometers, bordering on amorphous.

Auger spectroscopy in Fig. 15 of the sputtered anodized film shows the presence of iron (Fe), oxygen (O) and potassium (K)

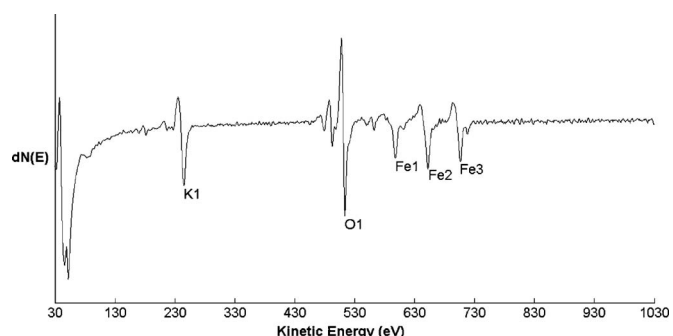


**Figure 15.** Auger spectroscopy analysis of the surface of 1010 steel anodized in 50% KOH solution indicates potassium (K) contamination in the surface film.

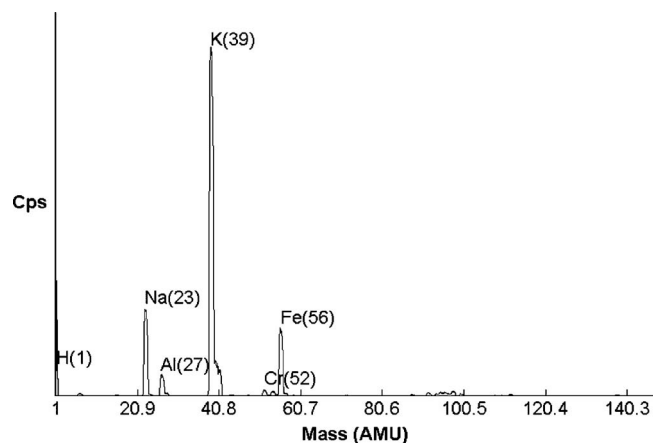


**Figure 16.** Secondary ion mass spectroscopy (SIMS) analysis of the surface of 1010 steel anodized in 50% KOH solution shows potassium (K) and iron (Fe) and a trace sodium (Na) in the anodized film.

throughout the film. The secondary ion mass spectroscopy (SIMS), in Fig. 16, agreed with the above Auger data, and also showed the presence of sodium (Na), in the anodic films grown in the KOH solutions.

The EIS results are shown in Fig. 17. The anodized magnetite film is apparently an electronic conductor and the film is practically invisible with EIS. Thermal heat treating the anodized film greatly improved the corrosion resistance as seen in the rise of the low frequency EIS curve. The anodized plus thermal treated film outperformed both the anodized-only and the thermal-treated-only steel as a barrier layer by having a very high polarization resistance at 0.1 Hz. The thermal-treated steel has no better corrosion resistance than the bare steel.

PDP tests in 3.5% NaCl were conducted on 1010 steel with different surface conditions, and are shown in Fig. 18. The anodized steel has greater resistance in saltwater than bare steel, but the anodized + heat-treated steel is even better.

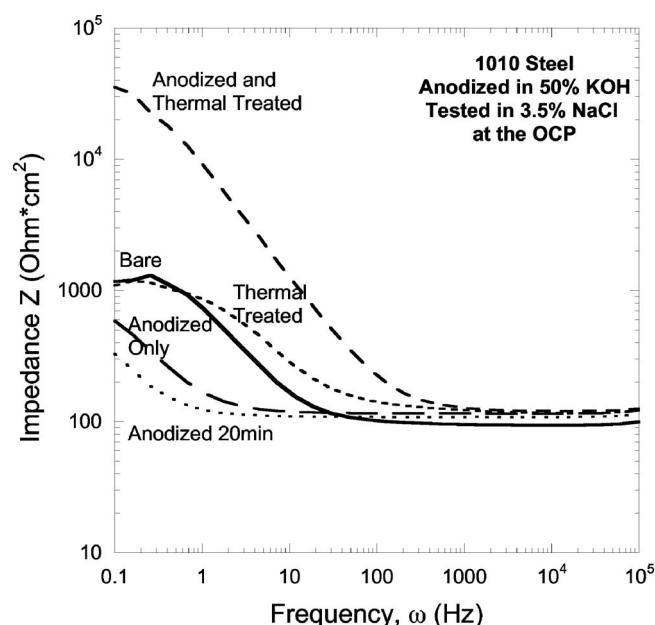


**Figure 17.** EIS tests show that the anodized 1010 steel sample surfaces were electrically conductive and became more electrically insulated (corrosion resistant) upon thermal treatment.

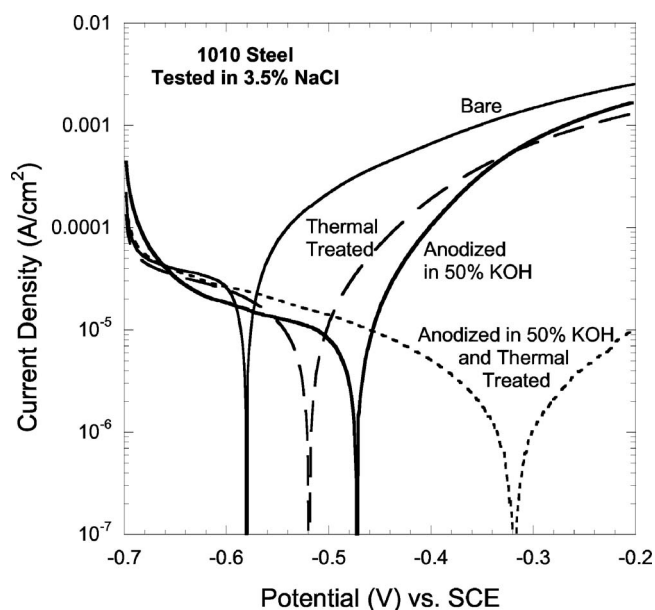


**Figure 18.** PDP tests in salt water of 1010 steel reveal the enhanced corrosion resistance of anodized and also the anodized plus thermally treated steel.

### Conclusion

It is possible to anodize steel in 10% to saturated solutions of KOH or NaOH. The anodized film is magnetite ( $\text{Fe}_3\text{O}_4$ ) with very fine crystallites. At higher voltages and temperatures, a semiadherent dichroic oxide is formed in which the surface color depends on the optical thickness and the viewing angle. There exist narrow regions of voltage and temperature where a thick, adherent oxide may be grown several microns thick on low carbon steel. These anodized films provide improved corrosion protection for steel and these are also suitable substrates for the bonding of organic coatings. Anodizing would also be a suitable factory process to place a protective patina on the weathering steels prior to service.

### Acknowledgments

We appreciate the contributions of Drew Prichard, Evan Prichard, Erica Herring, Kathleen Donovan, Maia C. Romanes, Lisa Zeeb, and Amanda McCleary. This research was financed in part by the U.S. Department of Energy, through WERC, a Consortium for Environmental Education and Technology Development. Equipment support was received from the New Mexico Tech Equipment Fund. A patent application has been filed for this anodizing process through the U.S. Patent and Trademark Office.

*New Mexico Tech assisted in meeting the publication costs of this article.*

### References

- H. E. Townsend, T. C. Simpson, and G. L. Johnson, *Corrosion (Houston)*, **50**, 546 (1994).
- E. Oberg and F. D. Jones, *Machinery's Handbook*, 18th ed., p. 2070, Industrial Press, New York (1968).
- U. S. Steel, *The Making, Shaping and Treating of Steel*, p. 991, Herbeck and Held, Pittsburgh, PA (1971).
- M. Pourbaix, *Atlas of Electrochemical Equilibria in Aqueous Solutions*, p. 644, NACE Cebelcor, Houston (1974).
- P. G. Joshi, G. Venkateswaran, K. S. Venkateswarlu, and K. A. Rao, *Corrosion (Houston)*, **49**, 300 (1993).
- L. A. Huchler, *Corrosion94*, NACE International, Baltimore (1994).
- H. L. Hollis, U.S. Pat. 621,084 (1899).
- H. L. Hollis, U.S. Pat. 664,550 (1900).
- H. L. Hollis, U.S. Pat. 827,802 (1905).
- J. A. McCarthy, U.S. Pat. 3,275,536 (1966).
- R. C. Bongartz and J. M. Belgay, U.S. Pat. 2,957,812 (1960).
- S. Fujimoto, T. Shibata, K. Wada, and T. Tsutae, *Corros. Sci.*, **35**, 147 (1993).
- S. Fujimoto, H. Nakatsu, S. Hata, and T. Shibata, *Corros. Sci.*, **38**, 1473 (1996).
- W. J. Baxter and D. W. Gorkiewicz, *Scr. Metall.*, **20**, 1169 (1986).
- S. Joiret, M. Keddad, X. R. Novoa, M. C. Perez, C. Rangel, and H. Takenouti, *Cem. Concr. Compos.*, **24**, 7 (2002).
- J. F. Jackovitz and G. A. Bayles, *Handbook of Batteries*, 2nd ed., D. Linden, Editor, p. 30.1, McGraw-Hill, New York (1995).
- W. M. Latimer, *The Oxidation States of the Elements and their Potentials in Aqueous Solutions*, 2nd ed., p. 227, Prentice-Hall, New York (1952).
- K. B. Blodgett, U.S. Pat. 2,587,282 (1952).
- W. A. Pliskin and E. E. Conrad, *IBM J. Res. Dev.*, **8**, 43 (1964).
- T. P. Ackerman and O. B. Toon, *Appl. Opt.*, **20**, 3661 (1981).
- CRC Handbook of Chemistry and Physics*, R. C. Weast, Editor, 56th ed., CRC, Cleveland, OH (1976).
- U. Schwertmann and R. M. Cornell, *Iron Oxides in the Laboratory*, 2nd ed., Wiley-VCH, New York (2000).
- M. F. Toney, T. C. Huang, S. Brennan, and Z. Rek, *J. Mater. Res.*, **3**, 351 (1988).
- B. D. Cullity, *Elements of X-Ray Diffraction*, 2nd ed., p. 102, Addison-Wesley, London (1978).
- R. M. Cornell and U. Schwertmann, *The Iron Oxides: Structure, Properties, Reactions, Occurrence and Uses*, VCH, New York (1996).